JAHU PLANE: DRAWINGS, MODEL AND STRUCTURAL ANALYSIS

De Aguiar, João B.

Sousa, Júlio C. S.

joao.aguiar@ufabc.edu.br

Universidade Federal do ABC

Av. Dos Estados, 5001, 09210-580, Santo André, SP, Brasil

De Aguiar, José M.

josemaguiar@gmail.com

Faculdade de Tecnologia de São Paulo – FATEC-SP - CPS.

Praça Coronel Fernando Prestes, 30 - CEP 01124-060, Bom Retiro, São Paulo, SP, Brasil

Abstract. *Jahu was the name of the first plane with a Brazilian crew to cross the Atlantic. The saga of such a voyage is described in the literature and well documented as the fact attracted large media coverage in the end of the years 1920. The hydroplane itself is not well known, however, mostly due to modifications introduced for the journey. Particulars of Jahu like its high weight, the use of a pair of external engines with propellers in opposite directions and large lateral floats, led people to call it the flying boat. Making this plane cross the ocean was in fact a dilemma, requiring a sequence of stops to solve problems; some caused by sabotage others by design. In this research, starting from the drawings of the plane, a model of the structure is constructed Flow equations are solved to infer the lift and drag forces in the structure of the aeroboat. Finite element equations are then used to determine response of the parts of the structure. Final results may help in the construction of a replica of the hydroplane undergoing in Italy.*

Keywords: *Modeling, Flow Formulation, Equilibrium Equations, FEA, Response*

INTRODUCTION

A hydroplane Savoia-Marchetti S.55, version C, constructed in Italy, reequipped with two 550 hp engines and enhanced floaters, was used by João Ribeiro de Barros and three other crew members, to cross the Atlantic South in 1927. Records of velocity and autonomy made the plane a preferred choice on those days. Jahu, as was named, was the first plane to cross in direct flight from Cape Verde, a Portuguese archipelago, to Fernando de Noronha, an island in northeast Brasil. This was the first time brazilians were able to cross the ocean in a plane /1/, /2/.

The first crossing of the south Atlantic in 1922 by Gago Coutinho and Sacadura Cabral inspired João Ribeiro, natural of Jau, interior of Sao Paulo state, to organize a raid with a brazilian crew. In fact, Gago Coutinho and Sacadura Cabral also helped João Ribeiro to plan the trip. However distant, the idea became possible after another pioneer of aviation, conde Casagrande with a Savoia-Marchetti S-55C named Alcyone, gave up a travel from Italy to Argentina, when only one fifth of the trip was completed. With the desistance, the Alcyone was returned to the SIAI, the manufacturer of the plane.

João Ribeiro, after understanding be the S-55 the most qualified to the endeavor, tried to buy a brand new airplane from SIAI, the maker of S-55 with no success. A selling offer for Alcyone was presented, instead. The deal was accepted after some proposed modifications to the S-55 were agreed upon. The plane received the name Jahu, Fig. 1, and in October, 1926 it took off from Genova. However only five hours after, the engines of Jahu started to present problems, and an emergency stop in Valencia, Spain, took place. Jahu´s crew ended up jailed, as landing was not authorized. Solved the case with diplomatic help, the plane flew to Gibraltar, where better conditions permitted the repairing of the engines, victims of sabotage.

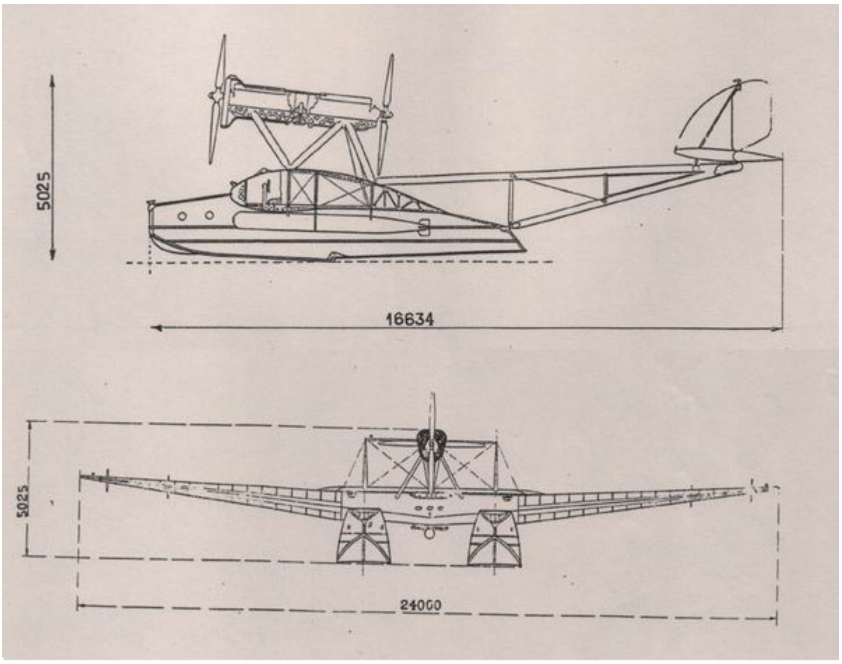

Fig. 1 Lateral and frontal view drawings of Jahu

In the next step of the flight, Canary Islands, in the Atlantic Ocean, were reached, again at the cost of great efforts from the crew. Failures in the fuel system of the engines required manual feeding. Solved the problem in the pumping system, trip continued. Next stop was in Praia, city in Cape Verde Islands, where the plane stayed for some time, to prepare for the most difficult part of the raid.

The stop in Praia was plagued by problems. Several modifications had to be implemented in order to face the most difficult part of the journey. Among them a change in pilot: a lieutenant from Sao Paulo had to be sent to Praia after the pilot refused to fly the plane again. After months on the stop, malaria fever accesses, general disbelief from public, João Ribeiro received an encouraging letter from his mother that made him go. Repaired, the hydro took off in April, 1927. During 12 hours it flew at an average velocity of 190 km/h and 250 m high to reach Fernando de Noronha, in a non-stop journey, a distance record in airplane on those days. It was a moment of great jubilee in Brazil. After that, trip followed along the Brazilian coast, and the cities of Natal, Recife, Salvador and Rio de Janeiro were visited. Trip ended in Sao Paulo in August of 1927. Jahu never flew again.

1 FORMULATION

In order to derive the kinematics and verify flight equilibrium, a set of equations relative to the motion of the air around the plane must be solved first, so as to determine the contact stresses in the skin of the plane. From the pressure-velocity field so obtained, the loading of the structure of the airplane may be inferred and stresses calculated to evaluate its response. In order to set up a perspective view of the problem, fundamental equations will be reviewed.

1.1 Flow Problem

Air flow around an airplane gives rise to the resultant contact stresses that actuate in its skin. In order to find these resultant efforts and its distribution, flow equations have to be solved. Therefore if a control volume V_c, with border surface S_c, is used to include the plane, flying with velocity $\mathbf{v}_p$, values of air flow variables in this volume maybe found from a set of conservation equations. These variables include the velocity $\mathbf{v}_a$, pressure p_a and temperature T_a. First equation is the conservation of mass $\dot{M}_a = 0$ /3/,

$$\frac{\partial}{\partial t}\int_{V_c} \rho_a \, dV + \int_{S_c} \rho_a \mathbf{v}_a \cdot \mathbf{n} dS = 0 \tag{1}$$

This is to say that the rate of increase of internal mass, first integral, plus the net rate of e-flux across the border of the control volume S_c, a large box in general, is zero. Here mass density of air is written as ρ_a. Control surface contains an inner part that contacts the plane S_c^p and another external, the outer border S_c^a, where free flow conditions apply, being

Proceedings of the XXXVIII Iberian Latin-American Congress on Computational Methods in Engineering
P.O. Faria, R.H. Lopez, L.F.F. Miguel, W.J.S. Gomes, M. Noronha (Editores), ABMEC, Florianópolis, SC, Brazil, November 5-8, 2017.

$S_c = S_c^p \cup S_c^a$. Control volume partition V_c^a has the volume occupied by the plane V_c^p deducted from total volume V_c. Although integrals could be described by their precise volumes or area partitions, this is not necessary as inside the plane air related quantities, are null.

Next pair of equations represents the conservation of the linear momentum $\mathbf{l}_a = \rho_a \mathbf{v}_a$, Eq. (2), and angular momentum $\mathbf{h}_a = \rho_a \mathbf{R}_a \times \mathbf{v}_a$ of the air surrounding the plane, Eq. (3):

$$\frac{\partial}{\partial t}\int_{V_c} \mathbf{l}_a \, dV + \int_{S_c} \mathbf{l}_a \, \mathbf{v}_a \cdot \mathbf{n} dS = \int_{V_c} \mathbf{b}_a \, dV + \int_{S_c} \{-p_a \mathbf{n} + \tau_a \, \mathbf{t}\} dS \tag{2}$$

$$\frac{\partial}{\partial t}\int_{V_c} \mathbf{h}_a \, dV + \int_{S_c} \mathbf{h}_a \; \mathbf{v}_a \cdot \mathbf{n} dS = \int_{V_c} \mathbf{R}_a \times \mathbf{b}_a \; dV + \int_{S_c} \mathbf{R}_a \times \{-p_a \mathbf{n} + \tau_a \, \mathbf{t}\} \, dS \tag{3}$$

In the upper equation, body forces are shown as $\mathbf{b}_a$, which include inertia forces, and surface tractions comprised by negative normal p_a and tangential τ_a. Symbol $\times$ is used to indicate the cross product between position vector $\mathbf{R}_a$, with respect to an inertial reference system $< X, Y, Z >$, and velocity vector $\mathbf{v}_a$ in the angular momentum expression $\mathbf{h}_a$. Scalar product is symbolized with a dot. If an airplane reference system $< x, y, z >$ is used, velocities above will be the relative ones.

First integral in right hand side of Eq. (2) represents the resultant body force, whereas the second one corresponds to the surface resultant. In both integrals, resultants over the plane are included, as they correspond to volume and surface integrals for the inner part. These resultants lead to the lift and drag forces over the airplane. Likewise, integrals in the right hand side of Eq. (3) indicate the corresponding moments, with respect to the reference system. These resultant vectors are required inputs for the structural problem. Energy conservation, that would couple the expressions, is not considered here.

1.2 Structural Problem

Kinematics of the airplane depends on the interaction with the air around it. For prescribed geometry of the plane, total weight $\mathbf{W}$ and thrust force $\mathbf{E}$, determined by the settings of the engine group and control surfaces, and pay load, interact with flow resultants. These actions have different directions and point of application, indicating the existence of resultant couples. The contact stresses over the surface of the plane, whose resultants are the lift vector $\mathbf{L}$ and the drag vector $\mathbf{D}$, define the other elements for the kinematics and stresses in the plane.

Newton's second law establishes that the rate of change of the linear momentum $\int_{V_c^p} \mathbf{l_p}\, dV$ equals the summation of external forces applied to the plane. Here $\mathbf{l}_p = \rho_p \mathbf{v}_p$ with the subscripts identifying plane quantities. Therefore

$$\frac{\partial}{\partial t}\int_{V_c^p} \mathbf{l}_p\, dV = \mathbf{W} + \mathbf{E} + \mathbf{L} + \mathbf{D} \tag{4}$$

being the lift vector perpendicular to the in-plane resultant. Taken the Z direction, with unit vector e_Z, as vertical and the resulting flow efforts as /4/:

$$\mathbf{F} = \int_{V_c^p} \mathbf{b}_a\, dV + \int_{S_c^o} \{-p_a\mathbf{n} + \tau_a \mathbf{t}\} dS \tag{5}$$

gives to lift and drag vectors the expressions:

$$\mathbf{L} = \mathbf{F}\cdot\mathbf{e}_k \tag{6}$$

$$\mathbf{D}_x = \mathbf{F}\cdot\mathbf{e}_x; \quad \mathbf{D}_y = \mathbf{F}\cdot\mathbf{e}_\mathbf{y} \tag{7}$$

where $< \mathbf{e}_x, \mathbf{e}_\mathbf{y} >$ are the in-plane unit vectors in x, y directions.

In the same form, the rate of change of the angular momentum $\int_{V_c^p} \mathbf{h}_p dV$ where $\mathbf{h}_p = \mathbf{R}_p \times \mathbf{v}_\mathbf{p}$ equals the summation of the moments of the external efforts:

$$\frac{\partial}{\partial t}\int_{V_c^p} \mathbf{h}_p dV = \sum_p \mathbf{M} \tag{8}$$

which comprises the moment resultant from air flow

$$\mathbf{M}_a = \int_{V_c^p} \mathbf{R}_p \times \mathbf{b}_a\, dV + \int_{S_c^a} \mathbf{R}_p \times \{-p_a\mathbf{n} + \tau_a\, \mathbf{t}\} dS \tag{9}$$

plus the contributions from external effort set $< \mathbf{W}, \mathbf{E} >$.

1.3 Finite Element Model

1.3.1 Principle of Virtual Work

Instead of using conservation laws directly to determine the flow characteristics, it is most expedient to use the principle of virtual work, PVW, in rate form, to the endeavor. This principle sets the rate of internal work to the rate of external work exchange /5/:

$$\int_{V_c} \delta\dot{\boldsymbol{\varepsilon}}_a{}^T \boldsymbol{\sigma}_a \, dV = \int_{V_c} \delta\mathbf{v}_a{}^T \mathbf{b}_a \, dV + \int_{S_c} \delta\mathbf{v}_a{}^T \{-p_a\mathbf{n} + \tau_a \mathbf{t}\} \, dS \tag{10}$$

where $\boldsymbol{\sigma}_a$ represents the Cauchy stress tensor, $\dot{\boldsymbol{\varepsilon}}_a$ is the strain rate tensor:

$$\dot{\boldsymbol{\varepsilon}}_a = \frac{1}{2}\{\nabla\mathbf{v}_a + \nabla\mathbf{v}_a{}^{\mathbf{T}}\} \tag{11}$$

being ∇ the gradient operator. Symbol δ indicates virtual quantities and matrix notation has been used.

Writing the velocity field in terms of its Cartesian components, $\mathbf{v}_a{}^T = \{\dot{u}_a, \dot{v}_a, \dot{w}_a\}$, where the set $< u_a, v_a, w_a >$ identifies the components of the displacement field, results in strain rate tensor $\dot{\boldsymbol{\varepsilon}}_a$ expressed in terms of $\mathbf{v}_a$ field. A linear operator $\boldsymbol{\mathcal{L}_a}$ relates both quantities as:

$$\dot{\boldsymbol{\varepsilon}}_a = \boldsymbol{\mathcal{L}_a} \mathbf{v}_a \tag{12}$$

Additionally, if inertia forces are separated from the set of body forces, $b_a = b_a^i + b_a^o$, renders virtual work expression, Eq. (10), in the form:

$$\int_{V_c} \delta\mathbf{v}_a{}^T \boldsymbol{L}_a{}^{\boldsymbol{T}} \boldsymbol{\sigma}_a dV - \int_{V_c} \delta\mathbf{v}_a{}^T \mathbf{b}_a^o dV - \int_{S_c} \delta\mathbf{v}_a{}^T (-p_a\mathbf{n} + \tau_a \mathbf{t}) dS = \int_{V_c} \delta\mathbf{v}_a{}^T \rho_a \mathbf{a}_a dV \tag{13}$$

being the accelerations dependent of time and position:

$$\mathbf{a}_a = \mathbf{v}_{a,t} + \nabla\mathbf{v}_a \, \mathbf{v}_a \tag{14}$$

Proceedings of the XXXVIII Iberian Latin-American Congress on Computational Methods in Engineering
P.O. Faria, R.H. Lopez, L.F.F. Miguel, W.J.S. Gomes, M. Noronha (Editores), ABMEC, Florianópolis, SC, Brazil, November 5-8, 2017.

The specific constitutive equation relating stresses to strain rates may now be included. For incompressible fluids, with moderate velocities involved, temperature coupling may be disconsidered and Navier-Stokes relationship assumed. This equation relates deviatoric components of stress to strain rates /6/:

$$\boldsymbol{\sigma}'_a = \boldsymbol{C}'_{\boldsymbol{\alpha}}\, \dot{\boldsymbol{\varepsilon}}_a ; \quad \boldsymbol{\sigma}'_a = \boldsymbol{\sigma}_a + p_a \mathbf{I} \tag{15}$$

where the deviatoric part $\boldsymbol{C}'_{\boldsymbol{a}}$ of the constitutive tensor $\boldsymbol{C}_{\boldsymbol{a}}$ depends on viscosity. Pressure is the negative trace of stress tensor $p_a = -tr\, \boldsymbol{\sigma}_a$ but it is not determined in the above equation. Meaning that an additional constitutive expression is necessary.

Upon introduction of the above relation, Eq. (15) into the expression of the PVW it results that:

$$\int_{V_c} \delta \mathbf{v}_a{}^T \boldsymbol{L}_{\boldsymbol{\alpha}}{}^T \boldsymbol{C}'_{\boldsymbol{\alpha}} \boldsymbol{L}_{\boldsymbol{\alpha}} \mathbf{v}_a \, dV - \int_{V_c} \delta \mathbf{v}_a{}^T \boldsymbol{L}_{\boldsymbol{\alpha}}{}^T p_a \mathbf{I} \, dV - \int_{V_c} \delta \mathbf{v}_a{}^T \mathbf{b}_a^o dV - \int_{S_c} \delta \mathbf{v}_a{}^{\mathbf{T}} \{-p_a \mathbf{n} + \tau_a \, \mathbf{t}\} dS = \int_{V_c} \delta \mathbf{v}_a{}^T \rho_a \mathbf{a}_a dV \tag{17}$$

being $\mathbf{I}$ the identity tensor. This equation may be solved numerically using spatial discretization by finite elements with time marching algorithms. In the process, internal variables are written in terms of nodal quantities by means of interpolation functions. Therefore, if the relations

$$\begin{aligned} \mathbf{v}_a &= \mathbf{N}^v \hat{\mathbf{v}}_a \\ p_a &= \mathbf{N}^p \hat{\mathbf{p}}_a \end{aligned} \tag{18}$$

are introduced into Eq. (17) and performed the algebra, it results that:

$$\mathbf{M}_a \frac{\partial}{\partial t} \hat{\mathbf{v}}_a + \{\mathbf{K}_l^v + \mathbf{K}_{nl}^v\} \hat{\mathbf{v}}_a + \mathbf{K}^p \hat{\mathbf{p}}_a = \mathbf{R}_V + \mathbf{R}_{\mathbf{s}} \tag{19}$$

where mass, velocity-stiffness – linear and non-linear, and pressure-stiffness matrices are:

$$\mathbf{M}_a = \int_{V_c} \mathbf{N}^{v^T} \rho_a \mathbf{N}^v dV \tag{20}$$

$$\mathbf{K}_l^v = \int_{V_c} \mathbf{B}^{v^T} \boldsymbol{C}'_{\boldsymbol{\alpha}} \mathbf{B}^v dV \tag{21}$$

$$\mathbf{K}_{nl}^{v} = \int_{V_c} \rho_a \mathbf{N}^{v^T} \{\nabla(\mathbf{N}^v \hat{\mathbf{v}}_a)^T\} \mathbf{N}^v dV \tag{22}$$

$$\mathbf{K}^{p} = \int_{V_c} \mathbf{B}^{v^T} \mathbf{I} \mathbf{N}^p dV \tag{23}$$

being $\mathbf{B}^v$ the strain-velocity interpolation matrix. Resultant vectors $\mathbf{R}_V$ and $\mathbf{R}_S$ represents the overall resultants of the body and surface forces, respectively.

1.3.2 Pressure Constraint

The discretized finite element system, Eq. (19), depends on the nodal velocities and pressures. Therefore, an additional equation has to be prescribed in order to complete the system to be solved in the flow problem. The remaining equation, conservation of mass, Eq. (1), may be used, in discretized form. Using the pressure as a virtual Lagrange multiplier, under stead state conditions, it writes as:

$$\int_{V_c} \delta p_a{}^T (\nabla^T \mathbf{v}_a) dV = 0 \tag{24}$$

because $div\, \mathbf{v}_a = \nabla^T \mathbf{v}_a = 0$. However as:

$$\begin{aligned} p_a &= \mathbf{N}^p \hat{p}_a \\ \nabla^T \mathbf{v}_a &= \mathbf{B}^v \hat{\mathbf{v}}_a \end{aligned} \tag{25}$$

it turns out that:

$$\mathbf{K}^{p^T} \hat{\mathbf{v}}_a = 0 \tag{27}$$

1.3.3 Airplane Equilibrium

Determination of velocity of the plane, stresses and deformations depends on the external actions derived in the flow solution. Returning to the equilibrium expression, Eq. (10), with the inclusion of the weight $\mathbf{W}$ and thrust $\mathbf{E}$, whose effect was not treated in the flow problem for simplicity, it results that:

$$\int_{V_p} \delta\mathbf{v}_p{}^T \boldsymbol{\sigma}_p dV = \int_{V_p} \delta\mathbf{v}_p{}^T \mathbf{b}_p dV + \int_{S_p} \delta\mathbf{v}_p{}^T \{-p_a \mathbf{n} + \tau_a \mathbf{t}\} dS + \delta\mathbf{v}_p{}^T \{\mathbf{W} + \mathbf{E}\} \tag{28}$$

This equation depends on the velocity of the airplane $\mathbf{v}_p$ and on the contact stresses on its surface, a function of the air velocity. Therefore Eq. (28) depends on the difference of velocities, i.e, the relative velocity.

Discretizing the space occupied by the airplane by volume elements, with required geometry, by means of interpolation functions N^v,

$$\mathbf{v}_p = N^v \hat{\mathbf{v}}_p \tag{29}$$

and considering the stress-strain relationship for the structural material given by:

$$\begin{aligned} \boldsymbol{\sigma}_p &= C_p \dot{\boldsymbol{\varepsilon}}_p \\ \dot{\boldsymbol{\varepsilon}}_p &= \mathbf{B}^v \mathbf{v}_p \end{aligned} \tag{30}$$

it turns out that:

$$\mathbf{M}_p \frac{\partial}{\partial t} \mathbf{v}_p + \mathbf{K}_p \mathbf{v}_p = \mathbf{R} \tag{31}$$

Here $\mathbf{R}$ stands for the sum of the external forces and $\mathbf{M}_p$ for the consistent mass –derived from the separation of the body forces into inertia and all others, $\mathbf{b}_p = \mathbf{b}_p^i + \mathbf{b}_p^o$. If constant velocity conditions are considered, the problem reduces to, at any instant, the solution of a simple system. From the solution, relative velocity field is found, and from it, stress and strain distribution on the plane. From the deformed shape, an iterative procedure may be devised to recalculate the flow problem as affected by the iteration fluid-structure.

1.4 Results

1.4.1 Drawings

Main parts of the Jahu are represented in the figures that follow, Figs. 2-5, based on the original drawings of the Savoia-Marchetti. These drawing were produced using SolidWorks™ /7/. Table 1 shows main characteristics of the plane.

Table 1 Main characteristics of Jahu

Maximum Wing Span	24 m
Maximum Length	16.75 m
Height	5.0 m
Wing Area	93.0 m^2
Aileron Surface Area	3.60 m^2
Horizontal Stabilizer Area	11.0 m^2
Vertical Stabilizer Area	4.40 m^2

In Fig.2 the tail group is shown. It includes the truss used to connect the stabilizers, horizontal and vertical, to the main body of the airplane. Structural elements include beam and shell components. Control surfaces are driven with a mechanism not shown. In Fig. 3, a drawing of the components of the wing set is included. Aerodynamic surfaces for low velocities are used along with longitudinal reinforcing elements. Wing is characterized by continuous diminishing of chord along the span.

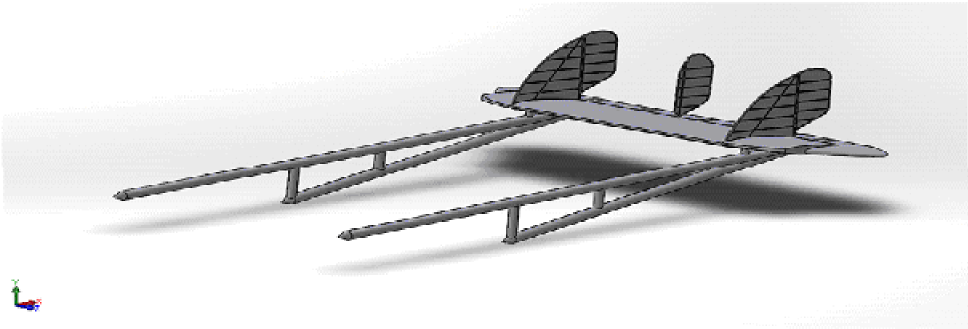

Fig. 2 Tail structure with supporting truss

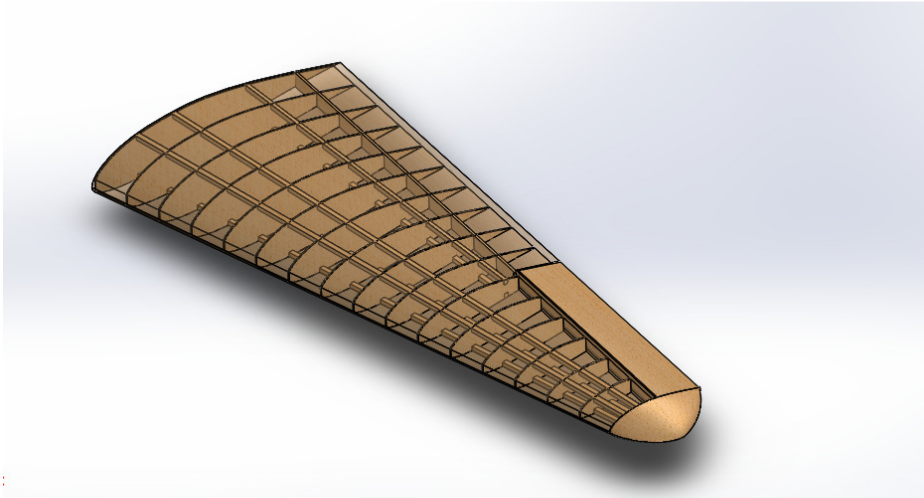

Fig. 3 Semi-wing structure drawing

Next pair of figures shows the remaining basic structural modulae of the plain. Fig. 4 shows the internal arrangement of boat unit, with transverse rings associated with longitudinal, main and secondary components. Fig. 5 is a drawing of the central unit, used to support the pair of engines that power the plane by means of a truss structure. This part is fixed in between the pair of boats.

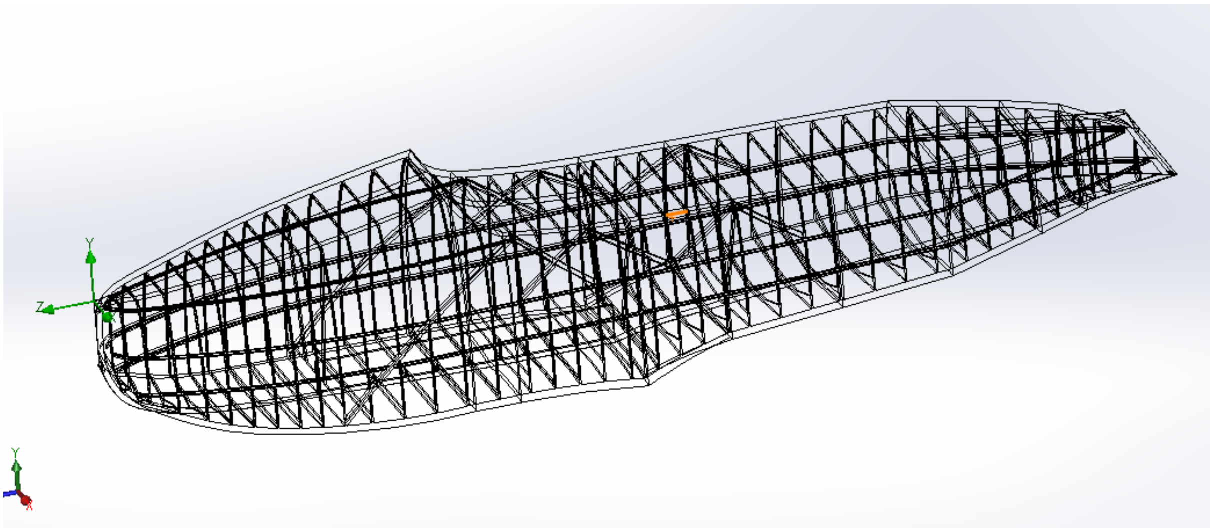

Fig. 4 Boat structural drawing

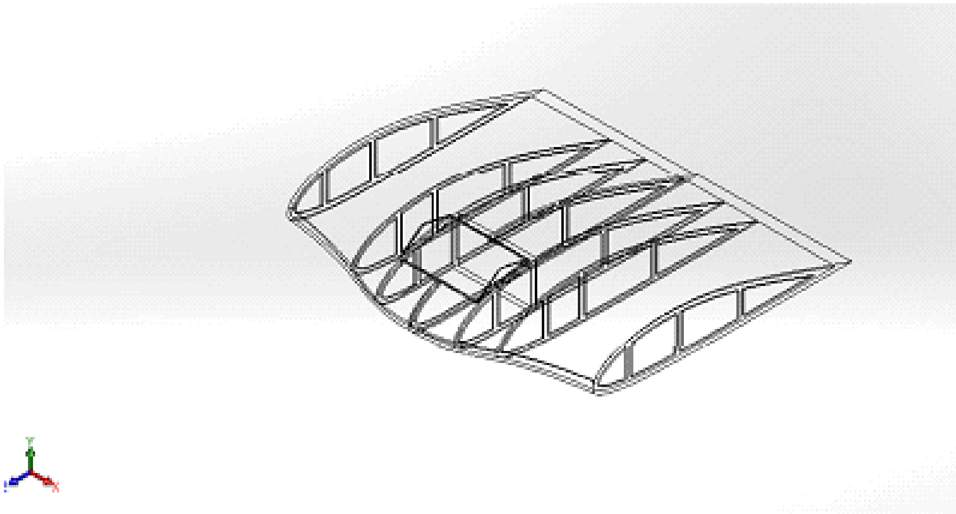

Fig. 5 Complete plane drawing

1.4.2 Flow Pattern

Velocity and height reached during trip trajectory by Jahu were quite low, reason why flow was approximately non-turbulent all over its skin. A part the region close to the propellers of the engines, not taken into account in the simulation, laminar conditions were found in most of the flow field around of the body of the hydro, Fig. 6. Flow processor of program SolidWorks was employed to the task. Level flight conditions were taken, under standard atmospheric conditions.

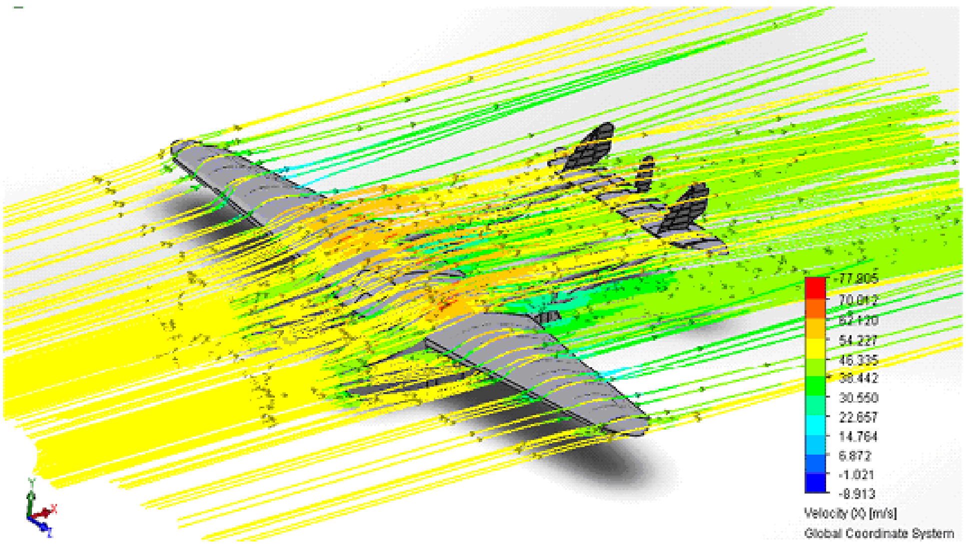

Fig. 6 Velocity field around the Jahu model

Pressure distribution in the flow problem is shown in Fig. 7, for the same conditions. From the plot it is seen that borders of attack of the outer wings have high pressures: peak values appear under these wings. Moreover, most of the drag in the plane comes out of the large boats, also crew space in the craft design.

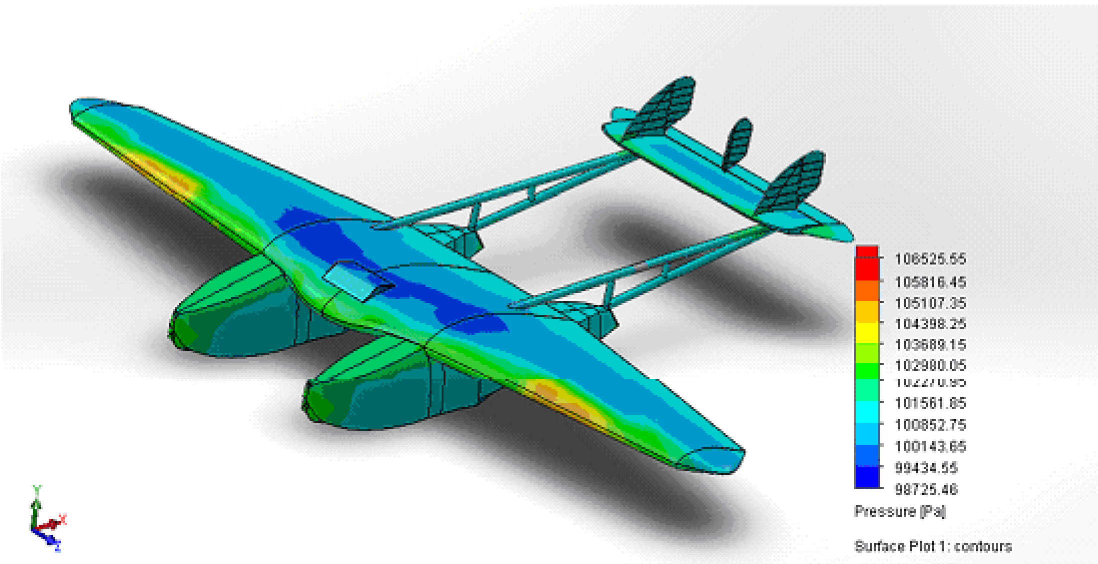

Fig. 7 Pressure distribution around the body of Jahu

1.4.3 Stress Field

Most stressed parts in the airplane are the wings and boat that served as fuselage also. Wing loading results basically from lift resultant obtained in the flow analysis. Primary, secondary and tertiary stresses are present in this part. A plot of equivalent Mises stresses is shown in Fig. 8. As primary and secondary structural members of Jahu were made up of wood. Combined with its shape it rendered a quite robust structure, but heavy. Structural arrangement of wings was shown in Fig. 3 confirm that structurally speaking, Jahu was a sound plane.

Under level flight, but with stabilizers at 3 degrees, top Mises stresses in the body of the plane were in the range of 50% of the yield stress, with higher values appearing in the boat area, Fig. 9. Wing loads, engines thrusts and weights transferred to the boats - scafos, by means of the central truss unit are responsible for that. Boats also received loading from the truss system of the tail stabilizers, Fig. 5.

Stress analysis used prismatic 3D elements of the library of program SolidWorks, with relative velocity field. Solution procedure included Newton method. No deformation correction to the loading was applied, as no solid-fluid interaction was pursued. Nonetheless this procedure is deemed unnecessary as the rigidity of the plane, a part its skin, so granted. Boat analysis under take off or sea descending was not considered as well. In this case skin friction with water, mostly, and air, less, would have to be considered.

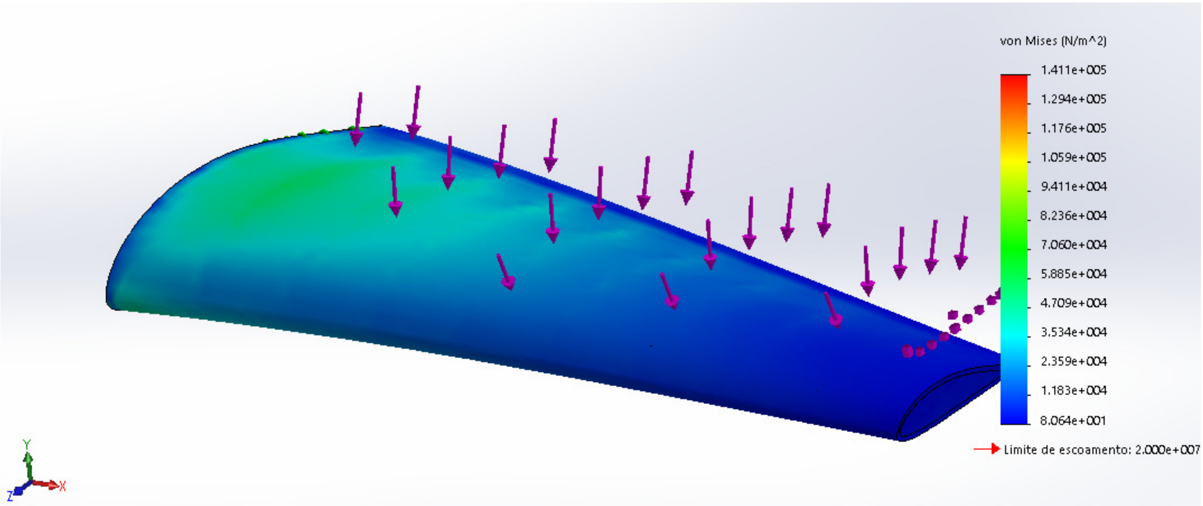

Fig. 8 Stress field in the outer wing model used for structural analysis

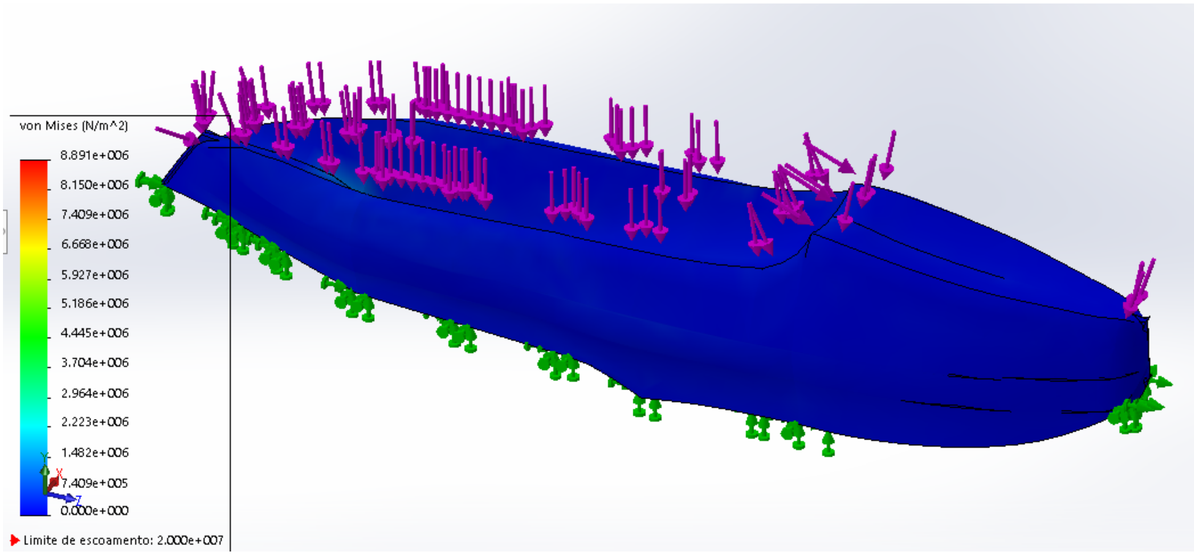

Fig. 9 Air-water loading and Mises stresses in the float unit

1.5 Discussion

Jahu had an unusual configuration of wings as it had to have a no zero attack angle at level flight. That could be at the cause of its form, size and weight. Table 2 presents obtained results from lift and drag forces.

Table 2 Flow analysis results

Variable	Symbol	Value
Drag Force, N	D	23.288 e+03
Lift Force, N	L	42.727 e+03
Drag Coefficient	C_D	0.055
Lift Coefficient	C_L	0.086

Values of the drag and lift coefficients, C_D and C_L, defined according to:

$$C_D = \frac{D}{\frac{1}{2}\rho_a A_f v_p{}^2} \tag{32}$$

$$C_L = \frac{L}{\frac{1}{2}\rho_a A_w v^2{}_p} \tag{33}$$

show large values but in the expected range for this type of plane. In the above expressions the areas used are the frontal A_f and projected A_w areas. Tail and main wings were considered. Values obtained for C_D are considered under estimated as the drag component D_E from the pair of engines was not taken into account.

1.6 Conclusions

A project is under way in Italy to construct and fly a replica of Savoia-Marchetti S-55, like Jahu, to South America. This is part due to the importance of the airplane to the history of aeronautics in Italy. A part this, Jahu is the last of such a series of planes. In the museum of TAM in Sao Carlos, Brazil, is the complete airplane, after restoration taken place in São Paulo with participation of Helipark /8/. This work is then a contribution to the understanding of design of such an important craft to the development of airplane industry.

It is seen that the airplane had some different concepts. Its aerodynamics shows large values of drag and lift coefficients that deemed the plane very consuming. Fact confirmed by the crew decision of dropping most of the equipment that came with the plane, in order to save space for the tanks of fuel. Lift obtained for zero attack angle was smaller than the weight of the plane, what confirmed the need for no zero attack angle in level flight.

Additional work is necessary to finish the structural analysis of the plane, incomplete at this point, but so far confirming the robustness of the plane. Investigations on alternative woods for construction of a lighter replica are important as well as powering considerations with reduction of emissions.

ACKNOWLEDGEMENTS

Progetto S55 /9/ help and cession of drawings used in the development of the model is dully acknowledged.

REFERENCES

/1/ https://pt.wikipedia.org/wiki/Jahu_(hidroavião)

/2/ *Idrovolante "Savoia Marchetti" tipo S. 55 X, Istbuzioni per il montaggio e per la regolaziche*

/3/ Gurtin, E., Continuum Mechanics, John Wiley, 2002

/4/ Simons, Martin, "Model Aircraft Aerodynamics", Special Interest Model Books, 4th edition, GB, 2006

/5/ Belytschko, T. and Fish, J., "A First Course in Finite Elements", John Wiley, 2010

/6/ Bathe, K. J., "Finite Element Procedures in Engineering Analysis", Prentice-Hall, 2nd Edition, 1996

/7/ SOLIDWORKS, Student's Guide to Learning, Dassault Systemes, 2013

/8/ www.helipark.net/index.php/pt/empresa/restauro-do-jahu

/9/ *Progetto S55 , Study Program 55, Busto Arsizio (Va), Italy, 2016*